Photon energy entanglement characterization by electronic transition interference

Alex Hayat*, Pavel Ginzburg, and Meir Orenstein

Department of Electrical Engineering, Technion, Haifa 32000, Israel
**ahayat@tx.technion.ac.il*

Abstract: We propose photon energy qubits and schemes for photon energy entanglement characterization. Bell inequality violation for energy qubits and complete Bell state analysis are demonstrated theoretically. Photon energy superposition state detection is performed by a two-photon absorption interferometer based on electron transition path interference. The scheme can be realized at room-temperature by two-level systems and semiconductor devices.

OCIS codes: (270.4180) Multiphoton processes; (270.5585) Quantum information and processing; (270.5565) Quantum communications

References and links:

1. A. Einstein, B. Podolsky, and N. Rosen, "Can quantum-mechanical description of physical reality be considered complete?" Phys. Rev. **47**(10), 777–780 (1935).
2. P. G. Kwiat, K. Mattle, H. Weinfurter, A. Zeilinger, A. V. Sergienko, and Y. Shih, "New high-intensity source of polarization-entangled photon pairs," Phys. Rev. Lett. **75**(24), 4337–4341 (1995).
3. T. Schmitt-Manderbach, H. Weier, M. Fürst, R. Ursin, F. Tiefenbacher, T. Scheidl, J. Perdigues, Z. Sodnik, C. Kurtsiefer, J. G. Rarity, A. Zeilinger, and H. Weinfurter, "Experimental demonstration of free-space decoy-state quantum key distribution over 144 km," Phys. Rev. Lett. **98**(1), 010504 (2007).
4. L. Lanco, S. Ducci, J. P. Likforman, X. Marcadet, J. A. W. van Houwelingen, H. Zbinden, G. Leo, and V. Berger, "Semiconductor waveguide source of counterpropagating twin photons," Phys. Rev. Lett. **97**(17), 173901 (2006).
5. A. B. U'Ren, R. K. Erdmann, M. de la Cruz-Gutierrez, and I. A. Walmsley, "Generation of two-photon States with an arbitrary degree of entanglement via nonlinear crystal superlattices," Phys. Rev. Lett. **97**(22), 223602 (2006).
6. J. S. Bell, "On the Einstein-Podolsky-Rosen Paradox," Physics **1**, 195 (1964).
7. J. D. Franson, "Bell's theorem and delayed determinism," Phys. Rev. D Part. Fields **31**(10), 2529–2532 (1985).
8. W. Tittel, J. Brendel, H. Zbinden, and N. Gisin, "Vlation of Bell inequalities by photons more than 10 km apart," Phys. Rev. Lett. **81**(17), 3563–3566 (1998).
9. J. D. Franson, "Bell inequality for position and time," Phys. Rev. Lett. **62**(19), 2205–2208 (1989).
10. J. Brendel, N. Gisin, W. Tittel, and H. Zbinden, "Pulsed Energy-Time Entangled Twin-Photon Source for Quantum Communication," Phys. Rev. Lett. **82**(12), 2594–2597 (1999).
11. P. G. Kwiat, A. M. Steinberg, and R. Y. Chiao, "High-visibility interference in a Bell-inequality experiment for energy and time," Phys. Rev. A **47**(4), R2472–R2475 (1993).
12. M. Halder, A. Beveratos, N. Gisin, V. Scarani, C. Simon, and H. Zbinden, "Entangling independent photons by time measurement," Nat. Phys. **3**(10), 692–695 (2007).
13. A. Cabello, A. Rossi, G. Vallone, F. De Martini, and P. Mataloni, "Proposed bell experiment with genuine energy-time entanglement," Phys. Rev. Lett. **102**(4), 040401 (2009).
14. S. Viciani, A. Zavatta, and M. Bellini, "Nonlocal modulations on the temporal and spectral profiles of an entangled photon pair," Phys. Rev. A **69**(5), 053801 (2004).
15. I. A. Khan, and J. C. Howell, "Experimental demonstration of high two-photon time-energy entanglement," Phys. Rev. A **73**(3), 031801 (2006).
16. A. K. Jha, M. Malik, and R. W. Boyd, "Exploring energy-time entanglement using geometric phase," Phys. Rev. Lett. **101**(18), 180405 (2008).
17. A. Hayat, P. Ginzburg, and M. Orenstein, "High-Rate Entanglement Source via Two-Photon Emission from Semiconductor Quantum Wells," Phys. Rev. B **76**(3), 035339 (2007).
18. A. Hayat, P. Ginzburg, and M. Orenstein, "Observation of Two-Photon Emission from Semiconductors," Nat. Photonics **2**(4), 238–241 (2008).
19. J. G. Rarity, and P. R. Tapster, "Experimental violation of Bell's inequality based on phase and momentum," Phys. Rev. Lett. **64**(21), 2495–2498 (1990).
20. K. V. Bayandin, and T. Martin, "Energy entanglement in normal metal–superconducting forks," Phys. Rev. B **74**(8), 085326 (2006).

#115553 - $15.00 USD Received 10 Aug 2009; revised 18 Oct 2009; accepted 1 Nov 2009; published 6 Nov 2009

21. S. Ducci, L. Lanco, V. Berger, A. De Rossi, V. Ortiz, and M. Calligaro, "Continuous-wave second-harmonic generation in modal phase matched semiconductor waveguides," Appl. Phys. Lett. **84**(16), 2974 (2004).
22. A. Hayat, P. Ginzburg, and M. Orenstein, "Infrared single-photon detection by two-photon absorption in silicon," Phys. Rev. B **77**(12), 125219 (2008).
23. F. Boitier, J.-B. Dherbecourt, A. Godard, and E. Rosencher, "Infrared quantum counting by nondegenerate two photon conductivity in GaAs," Appl. Phys. Lett. **94**(8), 081112 (2009).
24. Y. Silberberg, and D. Meshulach, "Coherent Quantum Control of Two-Photon Transitions by a Femtosecond Laser Pulse," Nature **396**(6708), 239–242 (1998).
25. D. Meshulach, and Y. Silberberg, "Coherent Quantum Control of Multiphoton Transitions by Shaped Ultrashort Optical Pulses," Phys. Rev. A **60**(2), 1287–1292 (1999).
26. L. Costa, M. Betz, M. Spasenović, A. D. Bristow, and H. M. van Driel, "All-optical injection of ballistic electrical currents in unbiased silicon," Nat. Phys. **3**(9), 632–635 (2007).
27. R. B. A. Adamson, L. K. Shalm, M. W. Mitchell, and A. M. Steinberg, "Multiparticle state tomography: hidden differences," Phys. Rev. Lett. **98**(4), 043601 (2007).
28. C. C. Gerry, "Two-photon Jaynes-Cummings model interacting with the squeezed vacuum," Phys. Rev. A **37**(7), 2683–2686 (1988).
29. A. Politi, M. J. Cryan, J. G. Rarity, S. Yu, and J. L. O'Brien, "Silica-on-silicon waveguide quantum circuits," Science **320**(5876), 646–649 (2008).
30. D. C. Hutchings, and E. W. Van Stryland, "Nondegenerate two-photon absorption in zinc blende semiconductors," J. Opt. Soc. Am. B **9**(11), 2065 (1992).
31. W. C. Hurlbut, Y.-S. Lee, K. L. Vodopyanov, P. S. Kuo, and M. M. Fejer, "Multiphoton absorption and nonlinear refraction of GaAs in the mid-infrared," Opt. Lett. **32**(6), 668–670 (2007).
32. A. Hayat, Y. Elor, E. Small, and M. Orenstein, "Phasematching in Semiconductor Nonlinear Optics by Linear Long-Period Gratings," Appl. Phys. Lett. **92**(18), 181110 (2008).
33. S. L. Braunstein, and A. Mann, "Measurement of the Bell operator and quantum teleportation," Phys. Rev. A **51**(3), R1727–R1730 (1995).
34. M. Michler, K. Mattle, H. Weinfurter, and A. Zeilinger, "Interferometric Bell-state analysis," Phys. Rev. A **53**(3), R1209–R1212 (1996).
35. J. A. W. van Houwelingen, N. Brunner, A. Beveratos, H. Zbinden, and N. Gisin, "Quantum teleportation with a three-Bell-state analyzer," Phys. Rev. Lett. **96**(13), 130502 (2006).
36. T. C. Wei, J. T. Barreiro, and P. G. Kwiat, "Hyperentangled Bell-state analysis," Phys. Rev. A **75**(6), 060305 (2007).
37. E. DelRe, B. Crosignani, and P. Di Porto, "Scheme for total quantum teleportation," Phys. Rev. Lett. **84**(13), 2989–2992 (2000).
38. M. O. Scully, B.-G. Englert, and C. J. Bednar, "Two-Photon Scheme for Detecting the Bell Basis Using Atomic Coherence," Phys. Rev. Lett. **83**(21), 4433–4436 (1999).
39. F. Boitier, A. Godard, E. Rosencher, and C. Fabre, "Measuring photon bunching at ultrashort timescale by two-photon absorption in semiconductors," Nat. Phys. **5**(4), 267–270 (2009).
40. B. E. Kardynał, Z. L. Yuan, and A. J. Shields, "An avalanche-photodiode-based photon-number-resolving detector," Nat. Photonics **2**(7), 425–428 (2008).
41. J. M. Fraser, and H. M. van Driel, "Quantum interference control of free-carrier density in GaAs," Phys. Rev. B **68**(8), 085208 (2003).
42. A. Hayat, P. Ginzburg, D. Neiman, S. Rosenblum, and M. Orenstein, "Hyperentanglement source by intersubband two-photon emission from semiconductor quantum wells," Opt. Lett. **33**(11), 1168–1170 (2008).

1. Introduction

Entanglement is one of the most curious phenomena in quantum mechanics contradicting the local realism of classical theories [1]. Moreover, the rapidly developing fields of quantum information processing and quantum computing rely on the ability to generate, characterize and utilize entanglement in various degrees of freedom. Many of the quantum information experiments employ photons as qubits, where the information encoding or entanglement is in polarization [2]. Photon polarization is stable in free-space propagation and is employed successfully for quantum key distribution [3] and entanglement swapping in free-space experiments. However in fiber-optical implementations the polarization state is randomly changed due to stress-induced birefringence. As photonic-based quantum information in fibers moves towards practical applications [4,5], more robust fiber-optical qubit realizations are required. Furthermore, a definitive test of Bell inequalities [6] calls for loophole-free experiments, including large space separation [7,8]. An important advancement in this direction was done by introducing time-energy entanglement for photons [9] or time-bin entangled photons [10], where characterization of such entanglement is typically performed via Franson interferometry (FI). The usual FI experiments require a reference energy of the photon pair (e.g. pump energy in parametric down-conversion) to be well-defined for reasonable time-resolution of the detectors employed [11,12]. Various improvements have

#115553 - $15.00 USD Received 10 Aug 2009; revised 18 Oct 2009; accepted 1 Nov 2009; published 6 Nov 2009

been reported in the characterization of energy-time entanglement using novel interferometers [13] or by employing spectral or temporal shaping of the photons [14], higher-dimensional entanglement [15], or geometric phase [16] which allows employing very broadband sources, however relying on photon polarization that can be unstable in fibers. A method for polarization-independent characterization of energy entanglement can be very useful for long-distance fiber-based quantum communication schemes.

2. Photon energy qubit detection by two-photon absorption interferometry

Recently, a compact electrically-driven and efficient source of energy-entangled photons operating at room-temperature was proposed [17], based on the newly-observed effect of semiconductor two-photon emission (TPE) [18]. The related photon energy qubits are very robust, however due to the relatively large fundamental energy uncertainty of such TPE-based sources, the use of FI is difficult. The major obstacle towards characterizing energy entanglement directly and employing energy qubits for quantum information is the difficulty of detecting energy superposition states:

$$\Psi = \cos\left(\frac{\theta}{2}\right)\left|\omega_2\right\rangle + \sin\left(\frac{\theta}{2}\right)e^{i\varphi}\left|\omega_1\right\rangle = \cos\left(\frac{\theta}{2}\right)\left|1\right\rangle_{\omega_2} + \sin\left(\frac{\theta}{2}\right)e^{i\varphi}\left|1\right\rangle_{\omega_1} \qquad (1)$$

where $\hbar\omega_{1,2}$ are two different energies and θ, φ are angles on the Bloch sphere (Fig. 1) .

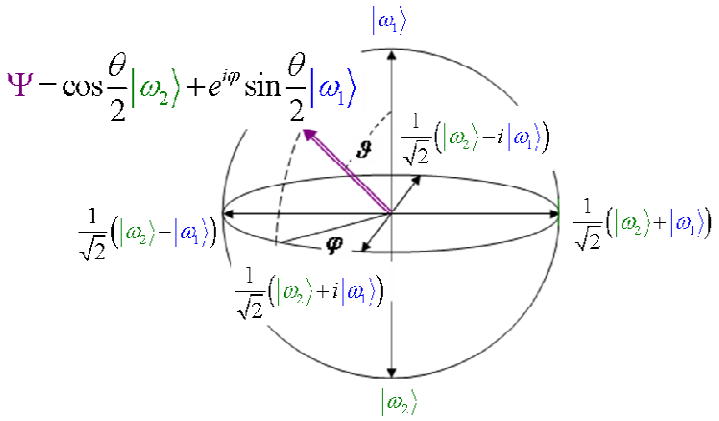

Fig. 1. Representation of an energy qubit on a Bloch sphere

Superconducting cooper-pair energy-entanglement tests were recently proposed by different-energy wavefunction interference in a Rarity-Tapster like interferometer [19] with energy difference small enough for the fringe measurement to be done on a time-scale much smaller than the beating period [20]. Nonetheless for room-temperature operating devices and detectors slower than a pico-second, such configurations are not realizable.

Here we propose a realizable scheme for direct characterization of photon energy entanglement at room temperature. The interferometry, usually done by photons, is performed here by electron transition amplitudes in a two-photon absorption (TPA) interferometer. The detection system is chosen so that neither of the photon energies in the energy qubit [Eq. (1)] is sufficient for the electron transition; and two auxiliary lasers with frequencies Ω_1 and Ω_2 are used for two interfering paths of TPA [Fig. 2(a)]. The auxiliary laser frequencies are low enough to prevent TPA and three-photon absorption of Ω_1 and Ω_2 alone, whereas the parasitic process of four-photon absorption is many orders of magnitude weaker and may be neglected. The two lasers must be mutually phase-locked for the interference to occur, e. g. generated from the same source by means of frequency conversion [Fig. 2(b)]. The proposed scheme can be realized in two-level atomic systems as well as in semiconductor photonic devices,

#115553 - $15.00 USD Received 10 Aug 2009; revised 18 Oct 2009; accepted 1 Nov 2009; published 6 Nov 2009

where frequency conversion (e.g. second harmonic generation - SHG) integrated in semiconductor hetero-structures was recently reported [21].

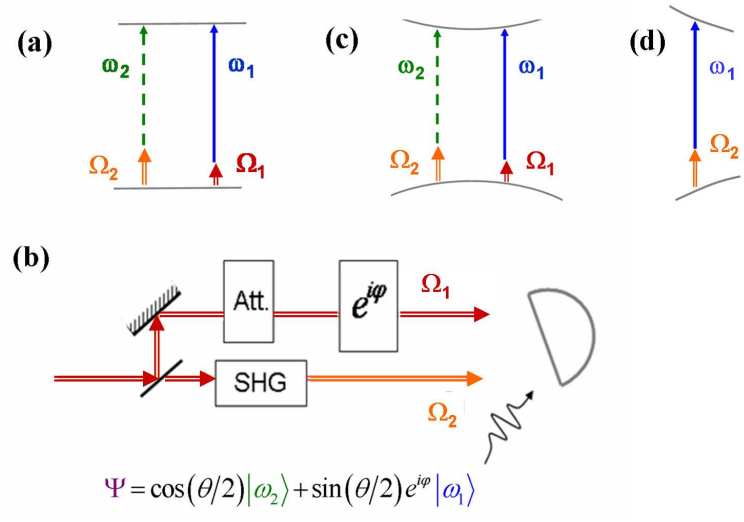

Fig. 2. Direct characterization of energy entanglement. (a) transition amplitude interference in TPA, (b) TPA interferometer realization scheme (c) semiconductor TPA interferometer implementation, (d) a parasitic TPA process of cross coupling possible in semiconductors at high electron crystal momentum.

Despite the different energy components in the detected photon ω_1 and ω_2, the transition energies for each path are complemented by the auxiliary frequencies $\Omega_1 + \omega_1 = \Omega_2 + \omega_2$, allowing transition amplitude interference. Constructive interference will result in a detection event with high probability, whereas destructive interference will not result in detection. Employing TPA with auxiliary lasers for efficient detection of low-energy photons was proposed involving practical room-temperature Si avalanche photodiodes [22], and realized recently experimentally in GaAs photomultipliers [23], while coherent-control of multi-photon effects was demonstrated in atomic systems [24,25] as well as in semiconductors [26]. In the configuration proposed here, the transition amplitude and the relative phase of each path in the TPA interferometer can be easily controlled by the relative phases and amplitudes of the auxiliary lasers, thus allowing the detection of any photon-energy qubit state covering the entire Bloch sphere (Fig. 1). In contrast to the momentum entanglement test setup limited to the equator of the Bloch sphere, this configuration allows an additional degree of freedom dismissing any rotational invariance loopholes in Bell inequality tests. Moreover, the three-dimensional energy qubit detection can be used for high-dimension quantum cryptography protocols (e.g. six-state) providing enhanced data security, and quantum state tomography [27] based on the complete two-level energy operator basis orthogonal under the Hilbert–Schmidt inner product defined here for energy:

$$E_z = \hbar\begin{pmatrix}\Delta & 0\\ 0 & -\Delta\end{pmatrix}\quad E_x = \hbar\begin{pmatrix}0 & \Delta\\ \Delta & 0\end{pmatrix}\quad E_y = \hbar\begin{pmatrix}0 & -i\Delta\\ i\Delta & 0\end{pmatrix}\quad E_0 = \hbar\begin{pmatrix}\Delta & 0\\ 0 & \Delta\end{pmatrix} \qquad (2)$$

where $\Delta = (\omega_1-\omega_2)/2$. $E_{x,y,z}$ are the SU(2) group generators of the energy space rotations with x, y and z representing the 'direction' of energy measurement.

For a given amplitude ratio and phase difference between the auxiliary lasers [Fig. 2(b)], any energy superposition [Eq. (1)] can be detected in the TPA interferometer. Therefore, two consecutive TPA interferometers detecting energy superpositions that are polar opposites on the Bloch sphere (Fig. 1), will project the photon state onto any energy-superposition basis with a dichotomic outcome (± 1) and in particular the four normalized energy operators

#115553 - $15.00 USD Received 10 Aug 2009; revised 18 Oct 2009; accepted 1 Nov 2009; published 6 Nov 2009

[Eq. (2)] $e_{x,y,z,0} = E_{x,y,z,0}/(\hbar\Delta)$. The two-photon Jaynes-Cummings interaction Hamiltonian of a TPA interferometer based on a two-level system is given by [28]

$$\hat{\mathrm{H}}_{\mathrm{int}} = i\hbar g_1\left[\sigma^+ a_1 b_1 - \sigma^- a_1^\dagger b_1^\dagger\right] + i\hbar g_2\left[\sigma^+ a_2 b_2 - \sigma^- a_2^\dagger b_2^\dagger\right] \tag{3}$$

where $g_{1,2}$ are the coupling constants for the two interfering transition paths, σ^+, σ^- are the electron energy level transition operators, $a_{1,2}$, $b_{1,2}$ and $a^\dagger_{1,2}$, $b^\dagger_{1,2}$ are the annihilation and creation operators of the fields in the two paths, where $a_{1,2}$ stand for the field of the photon at frequencies ω_1 and ω_2, while $b_{1,2}$ stand for the two auxiliary laser fields. The auxiliary laser electromagnetic fields are represented by coherent states: $|\alpha\rangle_{\Omega_i} = \sum_{n=0}^{\infty} \alpha_i^n \exp\left(-|\alpha_i|^2/2\right)/\sqrt{n!}\,|n\rangle_{\Omega_i}$ where $|\alpha_i|^2$ is the mean photon number in a coherent state at frequency Ω_i. The total transition matrix element is then $S = i\hbar g_1\alpha_1 \sin(\theta/2)e^{i\varphi} + i\hbar g_2\alpha_2 \cos(\theta/2)$ and the two-level destructive interference condition on the laser amplitudes and phases is:

$$g_2\alpha_2 / g_1\alpha_1 = -\tan(\theta/2)e^{i\varphi} \tag{4}$$

3. Bell inequality violation for energy qubits

TPA interferometry can be used for a variety of quantum information applications. Violation of Bell inequalities can be demonstrated by defining non-orthogonal energy basis for one TPA interferometer (A) measuring e_z and e_x for one photon of an energy-entangled pair, and the second TPA interferometer (B) measuring $e_{z'}$ and $e_{x'}$ for the second photon, with the primed energy axes rotated by $\pi/4$ radians. The TPA interferometer detection performs a projection onto a specific energy superposition (e.g. onto $|+\rangle = 1/\sqrt{2}\left(|1\rangle_{\omega_1} + |1\rangle_{\omega_2}\right)$ or $|-\rangle = 1/\sqrt{2}\left(|1\rangle_{\omega_1} - |1\rangle_{\omega_2}\right)$ states). Just as in the case of polarization-entangled photons, where the projection is performed onto a superposition in the horizontal/vertical basis, any energy entangled state can be written in the superposition basis - $|+\rangle, |-\rangle$. Therefore projection of one photon of the entangled pair onto one of the superposition states by applying the Hamiltonian from Eq. (3), projects the other photon onto a superposition with a well-defined amplitude and phase relation. For example, if one of the photons in the state $\Psi^+ = 1/\sqrt{2}\left(|1\rangle_{\omega_1}|1\rangle_{\omega_2} + |1\rangle_{\omega_2}|1\rangle_{\omega_1}\right)$ is rewritten in the $|+\rangle, |-\rangle$ basis $\Psi^+ = \frac{1}{2}\left[|+\rangle\left(|1\rangle_{\omega_2} + |1\rangle_{\omega_1}\right) + |-\rangle\left(|1\rangle_{\omega_2} - |1\rangle_{\omega_1}\right)\right]$ and measured in this basis yielding $|+\rangle$, the post-detection state of the second photon is in the pure state $\Psi_{post}{}^{+} = \frac{1}{\sqrt{2}}\left(|1\rangle_{\omega_2} + |1\rangle_{\omega_1}\right)$ and can be detected by a TPA interferometer. Similarly detection of a $|1\rangle_{\omega_1}$ for one photon in the $|1\rangle_{\omega_1}, |1\rangle_{\omega_2}$ basis will result in a pure state $\Psi_{post}{}^{+} = |1\rangle_{\omega_2}$. Such measurements are not restricted to the meridian and can be generalized to the entire Bloch sphere by including both e_x and e_y directions. Considering dichotomic outcomes of energy measurements in every direction resulting in + 1 and −1, Bell inequality for energy is defined as:

$$\left|\left\langle e_z^A e_{z'}^B\right\rangle + \left\langle e_x^A e_{z'}^B\right\rangle + \left\langle e_z^A e_{x'}^B\right\rangle - \left\langle e_x^A e_{x'}^B\right\rangle\right| \le 2 \tag{5}$$

#115553 - $15.00 USD Received 10 Aug 2009; revised 18 Oct 2009; accepted 1 Nov 2009; published 6 Nov 2009

For the test of Bell inequality based on energy entangled photons, one of the Bell states can be chosen e.g. $\Psi^{+} = 1/\sqrt{2}\left(|1\rangle^{A}_{\omega_1}|1\rangle^{B}_{\omega_2} + |1\rangle^{A}_{\omega_2}|1\rangle^{B}_{\omega_1}\right)$. The energy qubit TPA based detector for the first photon A performs energy measurements in two non-orthogonal energy basis e_z and e_x, namely the operators $e_z^A = \begin{pmatrix} 1 & 0 \\ 0 & -1 \end{pmatrix}$ and $e_x^A = \begin{pmatrix} 0 & 1 \\ 1 & 0 \end{pmatrix}$. For the second qubit B, the detector performs energy measurements in two rotated basis $e_{z'}$ and $e_{x'}$, namely the operators $e_{z'}^B = \begin{pmatrix} \cos\theta_1 & \sin\theta_1 e^{-i\varphi_1} \\ \sin\theta_1 e^{i\varphi_1} & -\cos\theta_1 \end{pmatrix}$ and $e_{x'}^B = \begin{pmatrix} \cos\theta_2 & \sin\theta_1 e^{-i\varphi_2} \\ \sin\theta_2 e^{i\varphi_2} & -\cos\theta_2 \end{pmatrix}$. The expectation values of the above operators acting on the Ψ^{+} state yield: $\left\langle e_z^A e_{z'}^B \right\rangle = -\cos\theta_1$, $\left\langle e_x^A e_{z'}^B \right\rangle = \sin\theta_1 \cos\varphi_1$, $\left\langle e_z^A e_{x'}^B \right\rangle = -\cos\theta_2$ and $\left\langle e_x^A e_{x'}^B \right\rangle = \sin\theta_2 \cos\varphi_2$, and by choosing $\theta_1 = \frac{3}{4}\pi, \varphi_1 = 0$, $\theta_1 = \frac{5}{4}\pi$ and $\varphi_2 = 0$, Bell inequality for energy [Eq. (5)] is violated for the energy-entangled states yielding the value of $2\sqrt{2}$.

This idealistic result is an upper limit on practical realizations, where detector efficiency plays a significant role in the visibility of the experimental result. In practical implementations, the TPA efficiency can be enhanced for long interaction lengths, strong spatial confinement and short temporal modes, e.g. by photon pulses propagating in waveguides [29].

Being a nonlinear process, two-photon absorption (TPA) efficiency is strongly dependent on the localization of light both spatially and temporally. Furthermore, relatively long propagation in a waveguide-based detector (~1mm) can significantly enhance the efficiency relative to the simple non-waveguiding detectors with ~1μm absorbing layers.

As a specific example, for a waveguide-based detector, a pulse width of ~10psec can be chosen - easily achievable with existing sources, as well as waveguide mode area of ~10μm^2. The auxiliary beam with a peak power of ~100W and 10psec pulse-width can be easily obtained from commercially available ultrafast lasers, and for the mode area of ~10μm^2 it corresponds to peak intensity of I_p~GW/cm^2. Assuming the single photon pulse perfectly overlaps the auxiliary-beam pulse, the attenuation coefficient for the single-photon pulse is given by βI_p, where β is the TPA coefficient. For typical semiconductor materials, such as GaAs, β ~20cm/GW [30]. Therefore for a waveguide length of L~1mm the probability of the single-photon absorption via TPA is 1-exp(-βI_pL) ~86%.

As mentioned in section 2, the auxiliary laser wavelengths a chosen to be sufficiently long to prevent TPA and three-photon absorption in an ideal system. However, even if three-photon absorption of the auxiliary lasers alone is not prevented by choosing proper wavelengths in a specific implementation, for the discussed peak intensity of I_p~GW/cm^2, and the three-photon absorption coefficient in GaAs of γ~0.3cm^3/GW^2 [31] and the length of L~1mm, three-photon absorption probability under the undepleted pump assumption is 1-exp(-γI_p^2L) ~3%. The process of four-photon absorption is much weaker and can be neglected. Dispersion induced phase walk-off in long waveguide-based devices without proper design could limit the efficiency. However, various phase-matching techniques in semiconductor waveguides have been developed and are widely used for nonlinear optics in semiconductors including: gratings [32], form birefringence [4], and modal phase-matching [21]. Employing a phase-matching design can lead to efficient TPA interferometry in devices with ~mm or even ~cm lengths.

4. Bell state analysis

Bell state analysis [33,34] is crucial for potential applications of quantum information based on energy entanglement including swapping and teleportation. A full Bell state analyzer (BSA) is able to distinguish between all four of the Bell states,

#115553 - $15.00 USD Received 10 Aug 2009; revised 18 Oct 2009; accepted 1 Nov 2009; published 6 Nov 2009

$$\Psi^{\pm} = 1/\sqrt{2}\left(|1\rangle^{U}_{\omega_1}|1\rangle^{D}_{\omega_2} \pm |1\rangle^{U}_{\omega_2}|1\rangle^{D}_{\omega_1}\right) \quad \Phi^{\pm} = 1/\sqrt{2}\left(|1\rangle^{U}_{\omega_1}|1\rangle^{D}_{\omega_1} \pm |1\rangle^{U}_{\omega_2}|1\rangle^{D}_{\omega_2}\right) \quad (6)$$

where the energy entangled photons are indexed by U and D – the "up" and "down" spatial modes of the BSA beamsplitter (Fig. 3). In the proposed scheme, the TPA interferometers $D_{3,4,5,6}$ are set to detect the zero phase superposition $|+\rangle$, whereas for the π phase superposition $|-\rangle$ these detectors are transparent due to the destructive interference of electron transition paths.

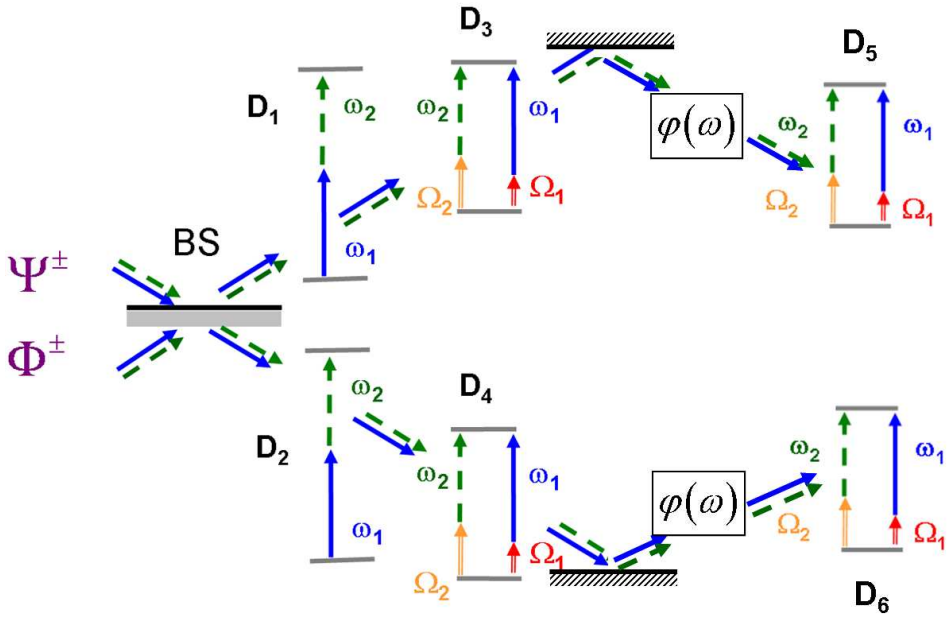

Fig. 3. Complete BSA scheme.

On the output of the beamsplitter the four Bell states [Eq. (6)] are transformed into

$$\begin{aligned}
\Psi^{+} &\rightarrow f_1 = 1/\sqrt{2}\left(|1\rangle^{U}_{\omega_1}|1\rangle^{U}_{\omega_2} - |1\rangle^{D}_{\omega_1}|1\rangle^{D}_{\omega_2}\right) \\
\Psi^{-} &\rightarrow f_2 = 1/\sqrt{2}\left(|1\rangle^{U}_{\omega_1}|1\rangle^{D}_{\omega_2} - |1\rangle^{D}_{\omega_1}|1\rangle^{U}_{\omega_2}\right) \\
\Phi^{+} &\rightarrow f_3 = 1/2\left(|2\rangle^{U}_{\omega_1} - |2\rangle^{D}_{\omega_1} + |2\rangle^{U}_{\omega_2} - |2\rangle^{D}_{\omega_2}\right) \\
\Phi^{-} &\rightarrow f_4 = 1/2\left(|2\rangle^{U}_{\omega_1} - |2\rangle^{D}_{\omega_1} - |2\rangle^{U}_{\omega_2} + |2\rangle^{D}_{\omega_2}\right)
\end{aligned} \quad (7)$$

For long propagation times, the phases of the different energy components would be different, however in TPA interferometers such accumulated phase difference can be easily calibrated by tuning the relative phase between the auxiliary lasers [Eq. (4)]. An anti-symmetric energy state Ψ^- must be in an antisymmetric spatial state with a photon in each output mode of the beamsplitter (f_2 in Eq. (7) resulting in coincidences between detectors on both sides of the beamsplitter. The state Ψ^+ results in both photons on one of the outputs of the beamsplitter (f_1) with different energies $\hbar\omega_{1,2}$ which are detected by TPA detectors D_1 or D_2 having electron transition energy of $\hbar\omega_1 + \hbar\omega_2$. These detectors are transparent for two photons having equal energies $f_{3,}f_4$ resulting from the states $\Phi^{\pm}$.

Practical photon counters are based on detectors containing more than one electron available for photon detection. A TPA interferometer based on two electrons acting as a two-

#115553 - $15.00 USD Received 10 Aug 2009; revised 18 Oct 2009; accepted 1 Nov 2009; published 6 Nov 2009

photon detector can be modeled as two one-electron TPA interferometers equally overlapping the photon mode - each one evolving under the Hamiltonian in Eq. (3) resulting in a projection onto an energy superposition of each one of the two photons. TPA interferometers containing more than one electron per degenerate energy state can detect two-photon states projecting them onto $\left|++\right\rangle^U = 1/\sqrt{2}\left(\left|1\right\rangle^U_{\omega_1} + \left|1\right\rangle^U_{\omega_2}\right)\otimes\left(\left|1\right\rangle^U_{\omega_1} + \left|1\right\rangle^U_{\omega_2}\right)$ by the projection operator $\hat{D}^U = \left|++\right\rangle^U\left\langle++\right|^U$ for the upper TPA interferometer, and $\hat{D}^D = \left|++\right\rangle^D\left\langle++\right|^D$ for the lower one, resulting in

$$\left\langle f_3\right|\hat{D}^U\left|f_3\right\rangle = 1/2\ \left\langle f_4\right|\hat{D}^U\left|f_4\right\rangle = 0\ \left\langle f_3\right|\hat{D}^D\left|f_3\right\rangle = 1/2\ \ \left\langle f_4\right|\hat{D}^D\left|f_4\right\rangle = 0 \qquad (8)$$

Therefore Φ^- will not result in detection in the TPA interferometers D_3, D_4. On the other hand Φ^+ results in a click in one of the two TPA interferometers D_3 or D_4 [Eq. (8)]. A dispersive element $\varphi(\omega)$ is set to introduce a π phase difference between the ω_1 and ω_2 energy components of the state f_4 converting it into f_3, which will be detected by the TPA interferometers D_5 or D_6. All four energy-entangled Bell states are therefore resolved by this BSA: D_3 or D_4 indicate Φ^+, D_5 or D_6 indicate Φ^-, D_1 or D_2 indicate Ψ^+, and coincidence between any of the detectors on both sides of the beamsplitter indicate Ψ^-. TPA in this scheme is the necessary nonlinear effect allowing full BSA in contrast to a partial BSA based on linear optics commonly used for photon polarization states and time bins [35], whereas full BSA by linear optics can be realized only for hyper-entangled photons [36]. TPA was proposed previously for polarization qubit BSA [37,38], and was used in second order photon correlation measurements [39].

The above description of a BSA is based on detector efficiency near unity, however practical detector efficiency is limited. Finite detection efficiency in resolving Ψ^- can cause a single detector click instead of a coincidence, however this can be solved by using photon number-resolving detectors that were implemented by commercial avalanche photodiodes recently [40]. Photon number resolving detectors D_3 and D_4 yield a two-photon signal for Φ^+ in contrast to one-photon signal for Ψ^-, while D_5 and D_6 yield a two-photon signal for Φ^- in contrast to one-photon signal for Ψ^-. Finite efficiency of D_3 or D_4 will not result in false detection of Φ^+ in D_5 or D_6 due to the destructive interference of the TPA interferometer. A false detection may occur only for the case of Ψ^+ not being detected by D_1 or D_2 and resulting in a two-photon signal in one of D_3, D_4, D_5 or D_6. For a one photon detection efficiency η_i of detector D_i,, the probability of BSA false detection (in one out of four Bell states only) is given by:

$$P = \frac{1}{8}\left[\left(1-\eta_1\right)\eta_3^{\,2} + \left(1-\eta_1\right)\left(1-\eta_3\right)^2\eta_5^{\,2} + \left(1-\eta_2\right)\eta_4^{\,2} + \left(1-\eta_2\right)\left(1-\eta_4\right)^2\eta_6^{\,2}\right] \qquad (9)$$

For detector efficiencies near 80% the false detection probability [Eq. (9)] is around 3%, and for higher efficiency the false detection probability becomes negligible.

5. Discussion and conclusion

The TPA interferometry scheme for quantum information based on energy qubits proposed here may be also employed in room-temperature semiconductor detectors [Fig. 2(c)]. However for semiconductor devices special care must be taken in order to avoid the TPA cross-coupling e.g. between $\Omega_2 + \omega_1$ due to the broad energy bands, enabling such transitions [Fig. 2(d)]. Various coherent control methods allow post selection of optically excited electrons by their crystal momenta or kinetic energy [26], however they require sub-psec carrier collection, which is very difficult. Carrier density control is more feasible; however it still suffers from low interference contrast [41]. The most practical method to mitigate TPA cross-couplings is the use of polarization selection rules [17,42], so that $\Omega_1 + \omega_1$ and $\Omega_2 + \omega_2$ absorption is allowed, whereas $\Omega_2 + \omega_1$ and $\Omega_1 + \omega_2$ is forbidden.

In conclusion, we have proposed a concept of photon energy qubits and presented approaches for characterization of photon energy entanglement including Bell inequality

#115553 - $15.00 USD Received 10 Aug 2009; revised 18 Oct 2009; accepted 1 Nov 2009; published 6 Nov 2009

violation and complete Bell state analysis. The detection of photon energy superposition states is allowed by the TPA interferometer introduced here, where the interferometry is performed by electron transition paths instead of photons. Realizations by atomic two-level systems and room-temperature semiconductor detectors appear feasible.

#115553 - $15.00 USD Received 10 Aug 2009; revised 18 Oct 2009; accepted 1 Nov 2009; published 6 Nov 2009